

Giant Core–Shell Nanospherical Clusters Composed of 32 Co or 32 Ni Atoms Held by 6 *p*-*tert*-Butylthiacalix[4]arene Units

Alexandre Gehin,[†] Sylvie Ferlay,^{*,†} Jack M. Harrowfield,[‡] D. Fenske,[§] Nathalie Kyritsakas,[†] and Mir Wais Hosseini^{*,†}

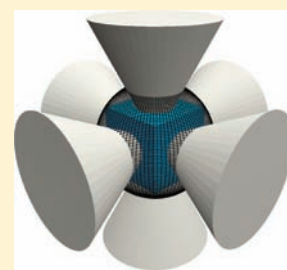
[†]Laboratoire de Chimie de Coordination Organique, UMR CNRS 7140, Université de Strasbourg, F-67000 Strasbourg, France

[‡]Laboratoire de Chimie Supramoléculaire, Institut de Science et d'Ingénierie Supramoléculaires, Université de Strasbourg, 8 allée Gaspard Monge, 67083 Strasbourg, France

[§]Institut für Anorganische Chemie, Universität Karlsruhe, D 76128 Karlsruhe, Germany

Supporting Information

ABSTRACT: Using combinations of *p*-*tert*-butylthiacalix[4]arene (TCA) and [M(DMSO)₆(BF₄)₂] salts (M = Co^{II} or Ni^{II}), two almost isostructural core–shell-type thermally stable giant nanoclusters, composed of 32 metal centers, 6 deprotonated calix units binding the metal centers by both their O and S atoms, 24 μ -oxo or μ -hydroxo bridging groups, and 6 MeOH molecules, have been prepared under mild and reproducible conditions. For both giant clusters, the oxidation state II [M^{II}₃₂O₁₆(OH)₈(CH₃OH)₆TCA₆ (M = Co or Ni)] for the metal center was demonstrated by X-ray photoelectron and electronic absorption spectroscopies.



INTRODUCTION

Polynuclear transition-metal compounds, in particular μ -oxo- and/or hydroxo-bridged polyoxometallate-type compounds, are of interest for their chemical and physical properties.¹ Several elegant strategies have been reported for the preparation of giant polynuclear species such as of, for example, iron,² molybdenum,³ manganese,⁴ and cadmium⁵ clusters.

The calix[4]arene backbone **1** (Figure 1, left)⁶ is an interesting unit for the design of polynucleating ligands. In

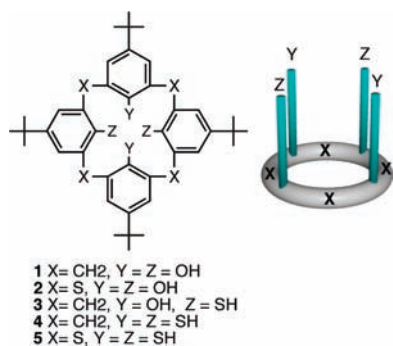


Figure 1. Chemical formulas of calix[4]arene, thiacalix[4]arene, and mercaptathiacalix[4]arene derivatives (left) and a schematic representation of their cone conformation (right).

particular, calix[4]arene derivatives in the cone conformation (Figure 1, right) offer four OH groups oriented in a convergent manner. This feature has been explored for the formation of koilands, which are face-to-face calix[4]arenes doubly fused by two Si^{IV},⁷ two Ti^{IV},⁸ one Si^{IV} and one Ti^{IV},⁹ two Al^{III},¹⁰ two Zn^{II},¹¹ two Eu^{III},¹² or four Nb^V¹³ ions.

The thiacalix[4]arene backbone **2**¹⁴ (TCA) for which the four CH₂ groups connecting the aromatic moieties are replaced by S atoms,¹⁵ and is a candidate of choice for the generation of high-nuclearity complexes. From **2**, which also adopts the cone conformation,¹⁶ tetranuclear copper(II)¹⁷ and tetra- and hexanuclear mercury(II)¹⁸ species have been generated. Using dimercapto-¹⁹ and tetramercaptocalix[4]arene derivatives²⁰ **3** and **4**, respectively, mono- and binuclear mercury(II) complexes have been reported. The synthesis and structural analysis of the tetramercaptotetrathiacalix[4]arene **5**²¹ and some mercury(II)¹⁸ and low-valence molybdenum and tungsten²² or iridium and rhodium²³ organometallic complexes have been also published.

The coordination ability²⁴ of **2** has been used for the preparation of other polynuclear species such as Cu₄,¹⁷ Mn₄,²⁵ Ln₄,²⁶ Ni₆,²⁷ V₆,²⁸ Fe₈,²⁹ Mn₄Ln₄,³⁰ Cu₉,³¹ Cu₁₀,³² and Co₂₄.³³ Recently, a new heterometallic cationic cluster [Co^{II}₂₄(M^{VI}O₄)₈TCA₆Cl₆]²⁺ combining 24 Co^{II} and 8 M^{VI} (M = Mo or W) atoms was published.³⁴ The highest-nuclearity homometallic clusters reported are those containing 32 Co³⁵ (Co^{II}₂₄Co^{III}₈O₂₄(OH)₂₄TCA₆) or Ni atoms (Ni^{II}₃₂(OH)₄₀TCA₆).²⁷

Here, we report on the synthesis, structural studies, thermal and X-ray photoelectron spectroscopy (XPS) characterization of two new core–shell nanospherical clusters composed of 32 Co^{II} or 32 Ni^{II} (Co₃₂ and Ni₃₂) held together by 6 *p*-*tert*-butylthiacalix[4]arenes.

Received: March 14, 2012

Published: April 19, 2012

EXPERIMENTAL SECTION

Preparation of Co₃₂. In a crystallization tube (1 cm diameter), exposed to the atmosphere and at room temperature, diffusion of a *N,N*-dimethylformamide (DMF) solution (5 mL) of Co(DMSO)₆(BF₄)₂ (230 mg, 0.28 mmol) into a DMF solution (1 mL) containing the thiacalixarene **2** (20 mg, 2.78 × 10⁻² mmol) and Et₃N (0.1 mL) provided a green solution after ca. 1 h. This was filtered before MeOH (1 mL) was carefully added. After 1 week, a fine pale-green precipitate had formed at the bottom of the tube. Upon standing further for ca. 3 weeks, large pink crystals, suitable for single-crystal X-ray diffraction, were formed on the wall of the tube. Yield: 97 mg (48%). MS [ESI, dimethyl sulfoxide (DMSO)]. Found: *m/z* 2285.7. Calcd for Co₃₂(TCA)₆(CH₃OH)₆O₁₆(OH)₈(KNa₂)³⁺: *m/z* 2285.6. IR (ν , cm⁻¹): 752.3, 1092.7, 1255.7, 1448.6, 1672.3, 2956.0.

Synthesis of Ni₃₂. In a crystallization tube (1 cm diameter), exposed to the atmosphere and at room temperature, diffusion of a DMF solution (5 mL) of Ni(DMSO)₆(BF₄)₂ (230 mg, 0.28 mmol) into a DMF solution (1 mL) containing the thiacalixarene **2** (20 mg, 2.78 × 10⁻² mmol) and Et₃N (0.1 mL) provided a green solution after ca. 1 h. This was filtered before MeOH (1 mL) was carefully added. After 1 week, a fine green precipitate had formed at the bottom of the tube. Upon standing further for ca. 3 weeks, large green crystals, suitable for single-crystal X-ray diffraction, were formed on the wall of the tube. Yield: 95 mg (ca. 45%). MS (ESI, DMSO). Found: *m/z* 3385.7. Calcd for Ni₃₂(TCA)₆(CH₃OH)₆O₁₆(OH)₈(LiH)²⁺: *m/z* 3385.6. Found: *m/z* 6788.2. Calcd for Ni₃₂(TCA)₆(CH₃OH)₆O₁₆(OH)₈Na⁺: *m/z* 6787.8. IR (ν , cm⁻¹): 750.3, 1058.9, 1257.6, 1438.9, 1666.5, 2958.9.

Physical Measurements. *Single-Crystal Studies.* Data were collected at 173(2) K on a Bruker APEX8 CCD diffractometer equipped with an Oxford Cryosystem liquid N₂ device, using graphite-monochromated Mo K α (λ = 0.71073 Å) radiation. For both structures, diffraction data were corrected for absorption. Structures were solved using SHELXS-97 and refined by full-matrix least squares on *F*² using SHELXL-97. The H atoms were introduced at calculated positions and not refined (riding model).³⁶ In the case of Ni₃₂, because of disorder of the solvent molecules, the SQUEEZE command was used.³⁷ CCDC 887436 and 877437 contain supplementary crystallographic data for the Co₃₂ and Ni₃₂ nanospheres, respectively. They can be obtained free of charge from the Cambridge Crystallographic Data Centre via www.ccdc.cam.ac.uk/datarequest/cif.

Powder X-ray Diffraction (PXRD) Studies. For both Co₃₂ and Ni₃₂ nanoclusters, PXRD diagrams for the crystalline and powdered materials were collected on a Bruker D8 diffractometer using monochromatic Cu K α radiation with a scanning range between 3.8 and 30° and a scanning step of 2°/min.

The desolvated forms of Co₃₂ and Ni₃₂ nanospheres [Ni₃₂(des) and Co₃₂(des)] were generated upon heating the sample at 170 °C, and the crystallinity was studied by PXRD. The thermal stability of Co₃₂ and Ni₃₂ nanoclusters was studied by first heating the powder to 300 °C and then measuring the PXRD patterns at room temperature.

Thermogravimetric Analysis (TGA) Studies. TGA measurements have been performed on powdered single-crystal samples of both Co₃₂ and Ni₃₂ nanoclusters using a Pyris 6 TGA Lab System (Perkin-Elmer), using a N₂ flow of 20 mL/min and a heating rate of 10 °C/min.

XPS Measurements. XPS measurements were performed on powdered single-crystal samples of both Co₃₂ and Ni₃₂ nanoclusters using a ThermoVGScientific photoelectron spectrometer equipped with a twin anode, providing both unmonochromated Al K α and Mg K α radiation (1486.6 and 1453.6 eV, respectively). The spectrometer, equipped with a multichannel detector, was used in the constant resolution mode with a pass energy of 20 eV. The total resolution of the system was estimated at 0.55 eV. Spectra were referenced to the aliphatic hydrocarbon C 1s signal at 285 eV.

Solid-State UV Measurements. UV/vis spectra were obtained on powdered samples of single crystals of Co₃₂ and Ni₃₂ nanoclusters

using a Shimadzu UV3600 spectrometer (data were recorded in the reflection mode using a 150 mm integrating sphere, with a resolution of 4 nm and a sampling rate of 300 nm/min).

IR Studies. IR spectra were recorded on powdered samples of single crystals of Co₃₂ and Ni₃₂ nanoclusters using a Perkin-Elmer RX1 spectrometer.

RESULTS AND DISCUSSION

Using the *p*-*tert*-butylthiacalix[4]arene **2** in its cone conformation (Figure 1), a reproducible synthetic procedure using identical conditions was established for the formation of giant clusters composed of 32 Co or 32 Ni atoms. The formation of these polynuclear assemblies displaying almost identical structures was achieved under mild conditions. Upon slow diffusion at room temperature of a DMF solution containing the tetrafluoroborate salt of Co^{II} or Ni^{II} into a DMF solution of the TCA **2** and Et₃N as the base, a powder was obtained, which upon standing in MeOH afforded pink and green crystalline materials in the case of Co and Ni, respectively (see the Experimental Section). It is worth noting that these species could only be produced when using [M^{II}(DMSO)₆(BF₄)₂] (M = Co or Ni) salts. Interestingly, the same type of crystalline material was obtained using EtOH or *i*-PrOH, however with much lower crystalline quality. Both clusters have been characterized by X-ray diffraction on single crystals. (a) Crystal data for Co₃₂: (C₄₀H₄₄O₄S₄)₆Co₃₂(CH₃OH)₆O₁₆(OH)₈, space group *P*₂₁/*n*, *a* = 24.7390(7) Å, *b* = 26.8037(7) Å, *c* = 32.6310(9) Å, β = 94.2370(10)°, *V* = 21578.4(10) Å³, *T* = 173(2) K, *Z* = 2, *D*_c = 1.112 g/cm³, μ = 1.371 mm⁻¹, 149389 collected reflections, 48887 independent [*R*(int) = 0.0463], GOF = 1.052; *R*₁ = 0.0909, *wR*₂ = 0.2687 for *I* > 2 σ (*I*) and *R*₁ = 0.1398, *wR*₂ = 0.3015 for all data. (b) Crystal data for Ni₃₂: (C₄₀H₄₄O₄S₄)₆Ni₃₂(CH₃OH)₆O₁₆(OH)₈, *M* = 6732.73, monoclinic, space group *P*₂₁/*n*, *a* = 24.5603(5) Å, *b* = 26.6097(6) Å, *c* = 32.2446(7) Å, β = 93.4090(10)°, *V* = 21035.9(8) Å³, *T* = 173(2) K, *Z* = 2, *D*_c = 1.040 g/cm³, μ = 1.557 mm⁻¹, 163687 collected reflections, 48655 independent [*R*(int) = 0.0852], GOF = 1.366; *R*₁ = 0.1074, *wR*₂ = 0.2613 for *I* > 2 σ (*I*) and *R*₁ = 0.2169, *wR*₂ = 0.2949 for all data.

In both cases, the diffraction data obtained were treated supposing the presence of discrete molecular entities with the formula (32M)(16O²⁻)(8OH⁻)(6C⁴⁺)(6CH₃OH). The giant clusters, with the longest distances between opposite CH₃ groups of ca 24.7 and of 23.7 Å for Co₃₂ and Ni₃₂ species, respectively, display almost identical connectivity patterns (Figure 2, left). Whereas for Co₃₂ [(32Co)(16O²⁻)(8OH⁻)(6TCA⁴⁻)(6CH₃OH)·3DMSO·3DMF] the solvent molecules (three DMF and three DMSO) could be localized, for Ni₃₂, because of disorder of the solvents, the structure was refined using the SQUEEZE procedure.³⁸

Thus, although both species crystallize in the same space group (*P*₂₁/*n*), because the solvent molecules could not be identified in the case of Ni₃₂, the two crystals may or may not be isomorphous. The overall assembly in both cases may be described as a cubic metallic core composed of 8 Co or Ni centers located within a shell composed of 24 metal cations (Co or Ni) held together by 6 deprotonated thiacalix 2⁴⁻ occupying the apexes of an octahedron and forming an organic envelope (Figure 2, right).

The aesthetically appealing structure of both clusters is rather complex. It will be described starting from its organic envelope and zooming toward its core.

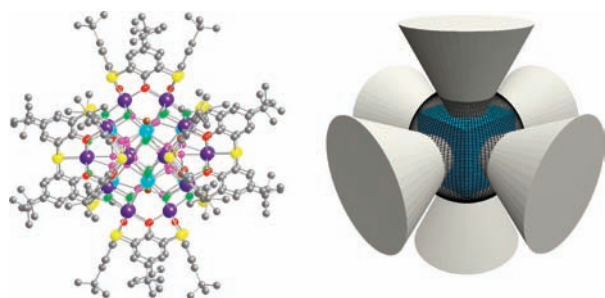


Figure 2. Crystal structure of the M_{32} ($M = \text{Co}$ or Ni) nanocluster. For the sake of clarity, the 8 core (light blue) and 24 shell (violet) metal centers are differentiated by color. The 24 O atoms of the calix units (red), 24 μ -oxo and μ -hydroxo units (green), and MeOH units (pink) are also differentiated by color. The C atom of the 6 MeOH molecules is colored brown. Solvent molecules are omitted (left), and a schematic representation of the giant M_{32} nanoclusters ($M = \text{Co}$ or Ni) composed of a cubic M_8 core (blue) inserted inside of a spherical M_{24} shell (black) surrounded by 6 thiacalix[4]arenes (gray) is shown (right).

As for the parent compound **2**,¹⁴ all (here, deprotonated) calix units (2^{4-}) adopt the cone conformation (Figure 1, right) with typical C–O distances in the 1.333(7)–1.368(8) and 1.281(13)–1.382(11) Å ranges for Co and Ni, respectively, and C–S distances in the 1.773(6)–1.804(8) and 1.705(17)–1.844(13) Å ranges for Co and Ni, respectively. Among the six calix units, the *tert*-butyl groups were found to be disordered over two positions (two calix with four and the remaining four with two disordered groups located on adjacent aromatic moieties). In the case of the Co_{32} cluster, the three DMF solvent molecules are located within the cavities of the six calix units but with an occupancy of 50%; i.e., one DMF molecule is disordered over two calix units. The three DMSO solvent molecules are located in the proximity of the metallic core with a $\text{Co}\cdots\text{O}$ distance of ca. 3.4 Å. One of them is disordered over two positions with an occupancy of 50%.

Each calix moiety behaves as a cluster keeper and binds four metal centers, forming a square through both of their phenoxide groups [O–M distance in the 2.022(4)–2.061(4) and 1.968(8)–2.060(9) Å ranges for Co and Ni, respectively] and their S atoms (S–M distance in the 2.4432(17)–2.4543(18) and 2.409(3)–2.439(3) Å ranges for Co and Ni, respectively). This motif is reminiscent of that found in the reported tetranuclear copper(II)¹⁷ and mercury(II)¹⁸ species (Figure 3).

The 6 tetranuclear M_4 units are further interconnected by 16 μ -oxo and 8 μ -hydroxo groups, forming thus a metallic shell of the sodalite type with a diameter of ca. 10.63 and 10.38 Å (longest M–M distance) for Co_{32} and Ni_{32} respectively. The protonation state of the above-mentioned bridging O atoms cannot be specified. The M–O distances are in the 2.031(5)–2.062(5) and 1.989(7)–2.061(6) Å ranges for Co and Ni, respectively. The coordination sphere around the metal centers is composed of five O and one S atoms. All metal centers adopt a distorted octahedral coordination geometry (Figure 4).

The metallic shell defines a cavity occupied by an octanuclear M_8 core. The 8 metallic centers occupying the corners of a distorted cube (M–M distance in the ca. 4.20–4.38 Å range) are connected to the shell through the 24 μ -oxo or μ -hydroxo bridging groups (three O atoms per metal center) with O–M distances in the 2.057(5)–2.323(14) and 1.989(7)–2.24(2) Å ranges for Co and Ni, respectively (Figure 5).

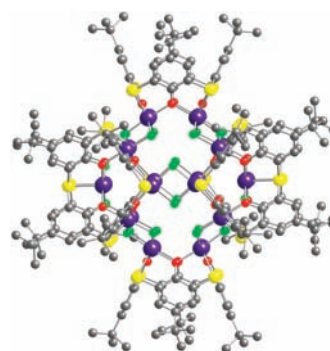


Figure 3. Portion of the crystal structure of the M_{32} ($M = \text{Co}$ or Ni) nanocluster showing the 24 metal centers (violet), forming the shell of the giant cluster held by the 6 thiacalix units. For the sake of clarity, the 24 O atoms of the calix units (red) and 24 μ -oxo and μ -hydroxo (green) are differentiated by color. Solvent molecules are omitted.

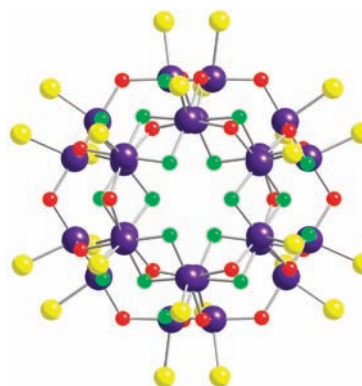


Figure 4. Portion of the crystal structure of the M_{32} ($M = \text{Co}$ or Ni) nanocluster showing the 24 metal centers (violet), forming the shell and their surroundings. The O atoms are differentiated by color (red and green) for clarity. Solvent molecules are omitted.

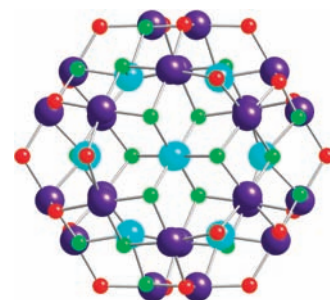


Figure 5. Simplified view of the M_{32} ($M = \text{Co}$ or Ni) nanocluster found in the crystal lattices, showing the 24 metal centers (violet), forming the sodalite-type shell, and the 8 metals (light blue), forming a cubic core located at the center of the giant cluster. The O atoms are differentiated by color (red and green) for clarity. Solvent molecules are omitted.

Finally, within the cubic core, the 8 metal centers are connected by 6 MeOH molecules, with M–O distances in the 2.169(14)–2.323(14) and 2.072(7)–2.39(2) Å ranges for Co_{32} and Ni_{32} , respectively.

With regard to the organic envelope and metallic shell, the two clusters are very similar, but they diverge in their cubic cores (Figure 6). For the Co_{32} cluster, of the six disordered MeOH molecules occupying the faces of the cubic arrangement, the O atoms of two of them are disordered over four

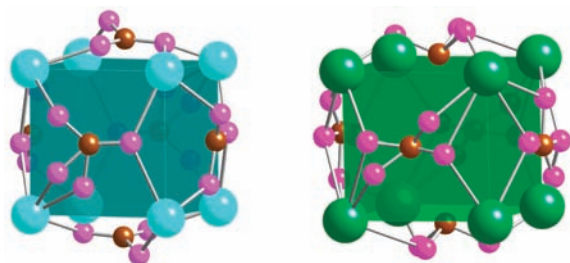


Figure 6. Portions of the crystal structures of the nanoclusters showing the Co_8 (left) and Ni_8 (right) cubic metallic core interconnected by six MeOH (disordered O atoms in pink and C atoms in brown). H atoms are omitted. For differences, see the text.

positions, whereas for the remaining four molecules, the O atoms are disordered over three positions (Figure 6, left). In the case of the Ni_{32} cluster, the reverse is observed (Figure 6, right).

In the Co species, the inner Co_8 unit atoms have a distorted octahedral O_6 coordination geometry, while in the Ni analogue, six have this form and two have distorted square-pyramidal O_5 coordination.

The packing of the two clusters is identical with no specific interactions between the polynuclear species (Figure S1 in the Supporting Information).

It is interesting to note that, for the reported analogous but mixed oxidation state Co cluster,³⁵ 48 μ -oxo or μ -hydroxo bridging anions are involved in the coordination sphere of the metal centers, whereas for the Ni analogue,²⁷ 40 μ -hydroxo groups were found to be bound to the metal. For both Co_{32} and Ni_{32} species reported here, in addition to 6 MeOH molecules bound to the metallic core, only 24 μ -oxo or μ -hydroxo groups are connected to metal centers.

The crystallization process used for the preparation of both Co- and Ni-based nanospheres led to single crystals attached to the walls and a powder deposited at the bottom of the tube. The crystals and powder were separated and dried in air. Both phases were analyzed using PXRD (Figures 7 and 8), and

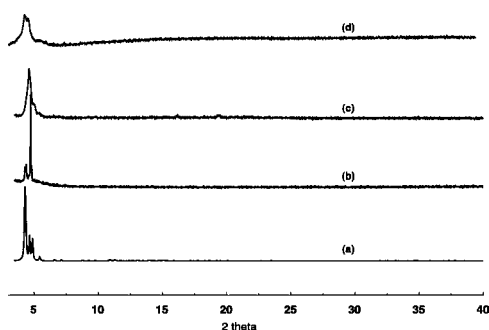


Figure 7. Comparison of the simulated (a) and recorded PXRD patterns for Co_{32} at room temperature (b), after heating at 170 °C (c), and after heating at 300 °C (d).

similar patterns were observed. For the Co_{32} nanosphere dried in air, the observed pattern (Figure 7b) fits well with the simulated one (Figure 7a). Interestingly, the powder sample heated at 170 °C to afford the desolvated material also displayed a similar pattern (Figure 7c, bottom), indicating conservation of the crystallinity of the sample. Retention of the same pattern even after heating at 300 °C (Figure 7d) showed

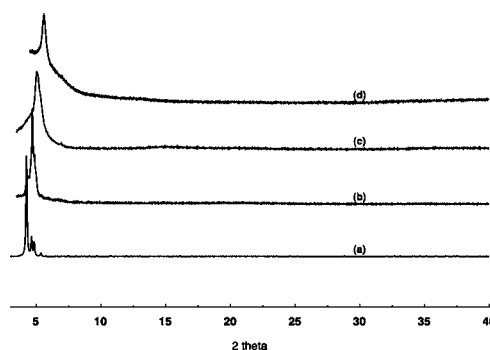


Figure 8. Comparison of the simulated (a) and recorded PXRD patterns for Ni_{32} at room temperature (b), after heating at 170 °C (c), and after heating at 300 °C (d).

the thermal stability of the sample. The same behavior was observed for the Ni_{32} nanosphere (Figure 8).

The thermal stability of both species was also investigated by TGA. For both Co_{32} and Ni_{32} species, in the 30–460 °C temperature range, a weight loss of ca. 25% was observed prior to decomposition, which appeared at 440 °C for Ni_{32} and at ca. 460 °C for Co_{32} (see Figure S2 in the Supporting Information). Although the weight loss prior to decomposition was assumed to be due to volatilization of the solvents, steps corresponding to the loss of different species were not discerned.

In order to clarify the oxidation state of the Co and Ni cations, XPS was used. Measurements were carried out on single crystals, using as reference salts $\text{Co}(\text{OH})_2 \cdot (\text{NO}_3)_2$ for Co_{32} and $\text{Ni}(\text{OH})_2 \cdot \text{SO}_4$ for Ni_{32} . For both Co_{32} (Figure 9, top) and Ni_{32} (Figure 9, bottom) giant clusters, the spectra displayed the $\text{M } 2p_{3/2}$, $\text{M } 2p_{1/2}$, and $\text{M } 2s$ signatures. Significantly, the match, in terms of binding energy and shape, between the recorded spectra for the two clusters and the corresponding reference compounds indicates that, in both

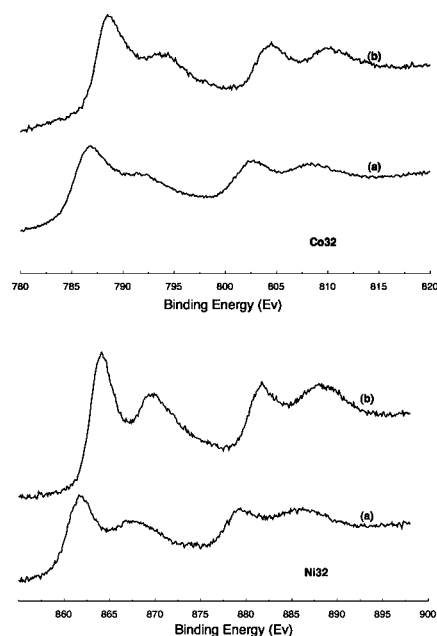


Figure 9. XPS of the polycrystalline samples Co_{32} (top, a) and Ni_{32} (bottom, a) exhibiting the $\text{M } 2p_{3/2}$, $\text{M } 2p_{1/2}$, and $\text{M } 2s$ signatures ($\text{M} = \text{Co}$ or Ni). The spectra are compared to those of $\text{Co}(\text{OH})_2 \cdot \text{SO}_4$ (top, b) for Co_{32} and $\text{Ni}(\text{OH})_2 \cdot (\text{NO}_3)_2$ (bottom, b) for Ni_{32} .

cases, the metal centers are in the oxidation state II with a deformed octahedral environment.

The UV/visible reflectance spectra of M_{32} ($M = \text{Co}$ or Ni) clusters were recorded in the solid state using polycrystalline samples (Figure 10). In agreement with the observations made

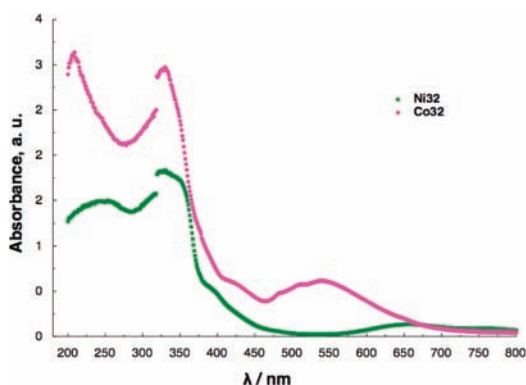


Figure 10. UV/vis reflectance spectra of Ni_{32} (green) and of Co_{32} (pink) recorded in the solid state at room temperature.

by XPS mentioned above, in both cases, the recorded spectra are typical of M^{II} species. For the Co_{32} giant cluster, considering the oxidation state II and an octahedral geometry, three transitions in the 250–800 nm region are expected. Indeed, three major bands at 320 nm, assigned to the ${}^4T_{1g}(\text{F}) \rightarrow {}^4T_{2g}(\text{F})$ transition, and at 550 nm, to the ${}^4T_{1g}(\text{F}) \rightarrow {}^4T_{1g}(\text{P})$ and ${}^4T_{1g}(\text{F}) \rightarrow {}^4A_{2g}(\text{F})$ transitions, were observed. For Ni_{32} , again considering a Ni^{II} cation in octahedral geometry, two transitions in the 250–800 nm region are expected and were indeed observed at 330 nm for the high-energy ${}^3A_{2g} \rightarrow {}^3T_{1g}(\text{P})$ transition and at 670 nm for the low-energy band assigned to the ${}^3A_{2g} \rightarrow {}^3T_{1g}(\text{F})$ transition. The presence of shoulders at ca. 400 nm probably results from the presence of M centers in a significantly deformed octahedral geometry, as discussed in the section dealing with structural analysis.

Finally, in support of the above-mentioned experimental facts, using the observed M–O or M–S distances, a bond-valence-sum (BVS) calculation³⁸ on both clusters revealed that for none of the metal centers was an oxidation state higher than 2.3 appropriate (see the Supporting Information).

CONCLUSIONS

A mild, reproducible procedure for obtaining thermally stable, giant core–shell nanoclusters containing 32 Co or Ni atoms enclosed by 6 tetrathiacalix[4]arene units has been established. The structure of both species was elucidated using X-ray diffraction techniques on both single-crystal and powdered crystalline samples. Both clusters are based on a cubic metallic core composed of 8 metal centers located in the center of a sodalite-type shell composed of 24 metals surrounded by 6 calix units as an organic envelope (Figure 2, right). In marked contrast with a reported analogous cluster,³⁵ obtained under hydrothermal conditions and which contains both Co^{II} and Co^{III} centers, for the Co_{32} and Ni_{32} clusters reported here, the metal centers are clearly in the oxidation state II.

Using the same methodology, the formation of analogous nanoclusters using other calixarene derivatives and metal centers is currently under investigation.

ASSOCIATED CONTENT

Supporting Information

TGA traces for Co_{32} and Ni_{32} as well as BVS calculations. This material is available free of charge via the Internet at <http://pubs.acs.org>.

AUTHOR INFORMATION

Corresponding Author

*E-mail: ferlay@unistra.fr (S.F.), hosseini@unistra.fr (M.W.H.).

Notes

The authors declare no competing financial interest.

ACKNOWLEDGMENTS

This work was financially supported by the University of Strasbourg (UdS), the Centre National de la Recherche Scientifique (CNRS), the Institut Universitaire de France (IUF), and the International Centre for Frontier Research in Chemistry (FRC), Strasbourg, France. Pierre Bernardt (LMSPC, Strasbourg, France) is warmly acknowledged for XPS measurements.

REFERENCES

- (1) (a) Fenske, D.; Ohmer, J.; Hachgenei, J. *Angew. Chem., Int. Ed. Engl.* **1985**, *24*, 993–995. (b) Liu, T.; Zhang, Y.-J.; Wang, Z.-M.; Gao, S. *J. Am. Chem. Soc.* **2008**, *130*, 10500–10501. (c) Alborés, P.; Rentschler, E. *Angew. Chem., Int. Ed.* **2009**, *48*, 9366–9370.
- (2) Taft, K. L.; Lippard, S. J. *J. Am. Chem. Soc.* **1990**, *112*, 9629–9630.
- (3) (a) Müller, A.; Kögerler, P. *Coord. Chem. Rev.* **1999**, *182*, 3–17. (b) Müller, A.; Roy, S. *Coord. Chem. Rev.* **2003**, *245*, 153–166. (c) Long, D. L.; Tsunashima, R.; Cronin, L. *Angew. Chem., Int. Ed.* **2010**, *49*, 1736–1758.
- (4) (a) Goldber, D. P.; Caneschi, A.; Delfs, C. D.; Sessoli, R.; Lippard, S. J. *J. Am. Chem. Soc.* **1995**, *117*, 5789–5800. (b) Bagai, R.; Christou, G. *Chem. Soc. Rev.* **2009**, *38*, 1011–1026.
- (5) Argent, S. P.; Greenaway, A.; Gimenez-Lopez, M.; Lewis, W.; Nowell, H.; Khlobystov, A. N.; Blake, A. J.; Champness, N. R.; Schröder, M. *J. Am. Chem. Soc.* **2012**, *134*, 55–58.
- (6) (a) Gutsche, C. D. *Calixarenes Revisited: Monographs in Supramolecular Chemistry*; Royal Society of Chemistry: Cambridge, U.K., 1998. (b) Asfari, Z.; Böhmer, V.; Harrowfield, J.; Vicens, J., Eds. *Calixarenes 2001*; Kluwer: Dordrecht, The Netherlands, 2001.
- (7) Delaigue, X.; Hosseini, M. W.; De Cian, A.; Fischer, J.; Leize, E.; Kieffer, S.; Van Dorsselaer, A. *Tetrahedron Lett.* **1993**, *34*, 3285–3288.
- (8) Olmstead, M. M.; Sigel, G.; Hope, H.; Xu, X.; Power, P. P. *J. Am. Chem. Soc.* **1985**, *107*, 8087–8091.
- (9) Delaigue, X.; Hosseini, M. W. *Tetrahedron Lett.* **1993**, *34*, 7561–7564.
- (10) Atwood, J. L.; Bott, S. G.; Jones, C.; Raston, C. J. *J. Chem. Soc., Chem. Commun.* **1992**, 1349–1351.
- (11) Atwood, J. L.; Junk, P. C.; Lawrence, S. M.; Raston, C. L. *Supramol. Chem.* **1996**, *7*, 15–17.
- (12) Bilyk, A.; Harrowfield, J. M.; Skelton, B. W.; White, A. H. *J. Chem. Soc., Dalton Trans.* **1997**, 4251–4256.
- (13) Corazza, F.; Floriani, C.; Chiesi-Villa, A.; Guastini, C. *Chem. Commun.* **1990**, 1083–1084.
- (14) Kumagai, H.; Hasegawa, M.; Miyanari, S.; Sugawa, Y.; Sato, Y.; Hori, T.; Ueda, T.; Kamiyama, H.; Miyano, S. *Tetrahedron Lett.* **1997**, *38*, 3971–3971.
- (15) Hosseini, M. W. In *Calixarenes 2001*; Asfari, Z., Böhmer, V., Harrowfield, J., Vicens, J., Eds.; Kluwer: Dordrecht, The Netherlands, 2001; pp 110–129.
- (16) Akdas, H.; Bringle, L.; Graf, E.; Hosseini, M. W.; Mislin, G.; Pansanel, J.; De Cian, A.; Fischer, J. *Tetrahedron Lett.* **1998**, *39*, 2311–2314.

- (17) Mislin, G.; Graf, E.; Hosseini, M. W.; Bilyk, A.; Hall, A. K.; Harrowfield, J. M.; Skelton, B. W.; White, A. H. *Chem. Commun.* **1999**, 373–374.
- (18) Akdas, H.; Graf, E.; Hosseini, M. W.; De Cian, A.; Bilyk, A.; Skelton, B. W.; Koutsantonis, G. A.; Murray, I.; Harrowfield, J. M.; White, A. H. *Chem. Commun.* **2002**, 1042–1043.
- (19) (a) Delaigue, X.; Hosseini, M. W.; Kyrtsakas, N.; De Cian, A.; Fischer, J. *Chem. Commun.* **1995**, 609–610. (b) Rao, P.; Enger, O.; Graf, E.; Hosseini, M. W.; De Cian, A.; Fischer, J. *Eur. J. Inorg. Chem.* **2000**, 1503–1508.
- (20) Delaigue, X.; Harrowfield, J. M.; Hosseini, M. W.; De Cian, A.; Fischer, J.; Kyrtsakas, N. *Chem. Commun.* **1994**, 1579–1580.
- (21) Rao, P.; Hosseini, M. W.; De Cian, A.; Fischer, J. *Chem. Commun.* **1999**, 2169–2170.
- (22) Buccella, D.; Parkin, G. *Chem. Commun.* **2009**, 289–291.
- (23) Hirata, K.; Suzuki, T.; Noya, A.; Takei, I.; Hidai, M. *Chem. Commun.* **2005**, 371–3720.
- (24) Kajiwara, T.; Iki, N.; Yamashita, M. *Coord. Chem. Rev.* **2007**, 251, 1734–1746.
- (25) (a) Desroches, C.; Pilet, G.; Borshch, S. A.; Parola, S.; Luneau, D. *Inorg. Chem.* **2005**, 44, 9112–9120. (b) Karotsis, G.; Teat, S. J.; Wernsdorfer, W.; Piligkos, S.; Dalgarno, S. J.; Brechin, E. K. *Angew. Chem., Int. Ed.* **2009**, 48, 8285–8288.
- (26) (a) Bi, Y. F.; Wang, X. T.; Liao, W. P.; Wang, X. W.; Deng, R. P.; Zhang, H. J.; Gao, S. *Inorg. Chem.* **2009**, 48, 11743–11747. (b) Bilyk, A.; Dunlop, J. W.; Fuller, R. O.; Hall, A. K.; Harrowfield, J. M.; Hosseini, M. W.; Koutsantonis, G. A.; Murray, I. W.; Skelton, B. W.; Sobolev, A. N.; Stamps, R. L.; White, A. H. *Eur. J. Inorg. Chem.* **2010**, 2127–2152.
- (27) Bilyk, A.; Dunlop, J. W.; Fuller, R. O.; Hall, A. K.; Harrowfield, J. M.; Hosseini, M. W.; Koutsantonis, G. A.; Murray, I. W.; Skelton, B. W.; Stamps, R. L.; White, A. H. *Eur. J. Inorg. Chem.* **2010**, 2106–2126.
- (28) Aronica, C.; Chastanet, G.; Zueva, E.; Borshch, S. A.; Clemente-Juan, J. M.; Luneau, D. *J. Am. Chem. Soc.* **2008**, 130, 2365–2371.
- (29) Desroches, C.; Pilet, G.; Szilágyi, P.; Molnár, G.; Borshch, S. A.; Bousseksou, A.; Parola, S.; Luneau, D. *Eur. J. Inorg. Chem.* **2006**, 357–365.
- (30) Karotsis, G.; Kennedy, S.; Teat, S. J.; Beavers, C. M.; Fowler, D. A.; Morales, J. J.; Evangelisti, M.; Dalgarno, S. J.; Brechin, E. K. *J. Am. Chem. Soc.* **2010**, 132, 12983–12990.
- (31) Karotsis, G.; Kennedy, S.; Dalgarno, S. J.; Brechin, E. K. *Chem. Commun.* **2010**, 3884–3886.
- (32) Kajiwara, T.; Kon, N.; Yokozawa, S.; Ito, T.; Iki, N.; Miyano, S. *J. Am. Chem. Soc.* **2002**, 124, 11274–11275.
- (33) Bi, Y. F.; Xu, G. C.; Liao, W. P.; Du, S. C.; Wang, X. W.; Deng, R. P.; Zhang, H. J.; Gao, S. *Chem. Commun.* **2010**, 6362–6364.
- (34) Bi, Y. F.; Du, S. C.; Liao, W. P. *Chem. Commun.* **2011**, 4724–4726.
- (35) Bi, Y. F.; Wang, X. T.; Liao, W. P.; Wang, X. F.; Wang, X. W.; Zhang, H. J.; Gao, S. *J. Am. Chem. Soc.* **2009**, 131, 11650–11651.
- (36) Sheldrick, G. M. *Program for Crystal Structure Solution*; University of Göttingen: Göttingen, Germany, 1997.
- (37) Spek, A. J. *Appl. Crystallogr.* **2003**, 36, 7–13.
- (38) Willis, A. S. Brown, I. *Valist*, version 3.0.15; CEA: Saclay, France, 1999.